Hindawi Publishing Corporation
Journal of Nanomaterials
Volume 2016, Article ID 8194516, 7 pages
http://dx.doi.org/10.1155/2016/8194516

Research Article

The Influence of Titanium Dioxide on Diamond-Like Carbon Biocompatibility for Dental Applications

C. C. Wachesk,[1] V. J. Trava-Airoldi,[2] N. S. Da-Silva,[3] A. O. Lobo,[1] and F. R. Marciano[1]

[1]*Laboratory of Biomedical Nanotechnology, University of Vale do Paraíba, São José dos Campos, SP, Brazil*
[2]*Associated Laboratory of Sensors and Materials, National Institute for Space Research, São José dos Campos, SP, Brazil*
[3]*Laboratory of Cell Biology and Tissue, University of Vale do Paraíba, São José dos Campos, SP, Brazil*

Correspondence should be addressed to F. R. Marciano; frmarciano@univap.br

Received 8 May 2016; Revised 15 August 2016; Accepted 23 August 2016

Academic Editor: P. Davide Cozzoli

The physical and chemical characteristics of diamond-like carbon (DLC) films make them suitable for implantable medical and odontological interests. Despite their good interactions with biological environment, incorporated nanoparticles can significantly enhance DLC properties. This manuscript studies the potential of titanium dioxide (TiO_2) incorporated-DLC films in dental applications. In this scene, both osteoblasts attachment and spreading on the coatings and their corrosion characteristics in artificial saliva were investigated. The films were grown on 304 stainless steel substrates using plasma enhanced chemical vapor deposition. Raman scattering spectroscopy characterized the film structure. As the concentration of TiO_2 increased, the films increased the osteoblast viability (MTT assay), becoming more thermodynamically favorable to cell spreading (W_{Ad} values became more negative). The increasing number of osteoblast nuclei indicates a higher adhesion between the cells and the films. The potentiodynamic polarization test in artificial saliva shows an increase in corrosion protection when TiO_2 are present. These results show the potential use of TiO_2-DLC films in implantable surfaces.

1. Introduction

Implantable surfaces probably have the main contribution for increasing the implant dentistry. Complex reactions at tissue-material interface settle the osseointegration and the long-term success of the implants [1]. Therefore, a surface modification to improve biocompatibility is mostly necessary [2]. In this scene, diamond-like carbon (DLC) coatings can reveal wear resistance, hardness, and corrosion resistance to a medical device surface [3–6]. These coatings consist of dense amorphous carbon or hydrocarbon and their mechanical properties fall between those of graphite and diamond [3, 4]. Some studies reported modified-DLC films improved biocompatibility, lubricity, stability, and cell adhesion [6, 7]. However, incorporated nanoparticles can change DLC performance according to the individual properties of each nanoparticle [8]. Yun et al. [5] related these characteristics to structural bonds [9], surface roughness [10], and whether the film is hydrophobic or hydrophilic.

A thin native oxide layer formed spontaneously on titanium surface caused by air, water, or any other electrolyte assigns titanium biocompatibility [11]. This layer is responsible for bone-bonding characteristics of titanium implants [12]. The photocatalytic nature of titanium dioxide (TiO_2) enables its use as antibacterial agent for decompose organisms [13–15]. These properties are strongly depending on the crystalline structure, morphology, and crystallite size [13, 15].

In the last recent years, previous manuscripts reported production and characterization of TiO_2-DLC films for biological applications [15–17]. However, besides the cytotoxicity, odontological applications also depend on the corrosion resistance [1, 18, 19]. A hostile electrolytic environment, as the mouth, causes gradual degradation of metallic biomaterials by electrochemical attack [20]. This manuscript studies the potential of TiO_2-DLC films in dental applications. In this scene, both osteoblasts attachment and spreading on the coatings and their corrosion characteristics in artificial saliva were investigated.

2. Experimental Procedures

The 304 stainless steel (10 mm × 10 mm × 1 mm) was the substrates. DLC and TiO_2-DLC films were deposited using plasma enhanced chemical vapor deposition to a thickness of around 2.0 μm [17]. Hexane was the feed gas to produce DLC films. Dispersions of TiO_2 (Aeroxide® from Evonik), in anatase crystalline form (average particle size of 17 nm), in hexane (0.1 and 0.5 g/L), substitute hexane to produce TiO_2-DLC films.

Raman scattering spectroscopy (Renishaw 2000 system with an Ar^+-ion laser (λ = 514 nm) in backscattering geometry) analyzed the atomic arrangement of the films.

All animal procedures were in agreement with guidelines of the Research Ethics Committee of the School of Dentistry in São José dos Campos (027/2008-PA/CEP). Enzymatic digestion harvested cells from newborn (2–4 days) Wistar rat calvaria [21]. The cells were plated on samples in 24-well polystyrene plates (density of 2×10^4 cells/well) using α-MEM (Gibco), supplemented with 10% fetal bovine serum (Gibco), 50 mg/mL gentamicin (Gibco), 5 μg/L ascorbic acid (Sigma), and 7 mM β-glycerophosphate (Sigma). During the experiments, cells were incubated (37°C) in a humidified atmosphere (5% CO_2) and the medium was changed every three days. The inverted microscope (CK40 Olympus) examined the progression of cultures.

The cell viability assay monitors the response and health of cells quantifying the mitochondrial activity by analyzing formazan crystals formed by reducing the salt 3-[(4,5-dimethylthiazol-2-yl)-2,5-diphenyltetrazolium bromide] (MTT) (Sigma-Aldrich). After treatment, 0.5 mg/mL of MTT was added to the cultures, which were incubated for 1 h (37°C), followed by 30 min gentle agitation in 200 mL of dimethyl sulfoxide. ELISA Spectracount Reader (Packard Instrument) with a 570 nm filter read the plates.

Phosphate-buffered saline (PBS) washed the cells. They were incubated for 10 min at room temperature with 300 nM 4′,6-diamidino-2-phenylindole and dihydrochloride (DAPI; Molecular Probes). For fixing, 200 mL paraformaldehyde (Sigma-Aldrich) at 4% was added to the wells and the plate incubated at room temperature for 10 min. Fluorescence microscope (DMLB Leica) examined the cells and a digital video camera (Leica DFC 300 FX) took the images.

One-way ANOVA (Graph Pad Prism 6®) analyzed the statistical differences. The populations from stainless steel, DLC, and TiO_2-DLC films were obtained with normal distribution and independent to each experiment. Statistical differences pointed out P values less than 0.05.

A sessile drop method with a Kruss EasyDrop (DSA 100) measured the contact angle (θ) of the samples. According to Owens method [22], the contact angle values with two different liquids (distilled water and diiodomethane) calculated the surface energy. Thermodynamically, the adhesion and spreading of cells from a liquid suspension onto solid substrata can be described by $W_{Ad} = \gamma_{CS} - \gamma_{CL} - \gamma_{SL}$ [23], where W_{Ad} is the interfacial free energy of adhesion, γ_{CS} is the cell-solid interfacial free energy, γ_{CL} the cell-liquid interfacial free energy, and γ_{SL} is the solid-liquid interfacial free energy, respectively. If W_{Ad} is negative, cell spreading is energetically favorable; while if W_{Ad} is positive, cell spreading is thermodynamically unfavorable.

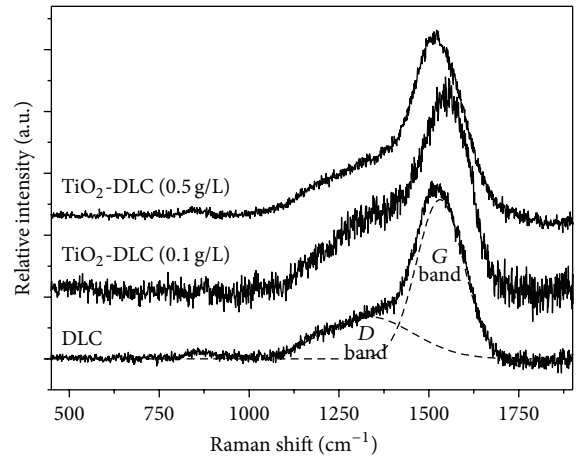

Figure 1: Raman spectra from DLC and TiO_2-DLC films. The spectra are vertically shifted for easy of comparison.

A conventional three-electrode cell performed the electrochemical tests. In this cell, a saturated Ag/AgCl electrode was the reference electrode, platinum wire was the counter electrode, and the stainless steel, DLC, and TiO_2-DLC films were the working electrodes. The working electrode exposed area was 0.5 cm^2. The electrolyte solution was a modified Fusayama artificial saliva [24], which consisted of NaCl (400 mg/L), KCl (400 mg/L), $CaCl_2 \cdot 2H_2O$ (795 mg/L), $NaH_2PO_4 \cdot H_2O$ (690 mg/L), KSCN (300 mg/L), $Na_2S \cdot 9H_2O$ (5 mg/L), and urea (1000 mg/L). The electrolyte was adjusted to pH 6.3 by either lactic acid or sodium hydroxide and maintained at 37°C. Potentiodynamic tests were carried out by polarization of samples in the anodic direction, from –1.0 to +1.0 V, just after exposition to the electrolyte solution. The potential sweep rate was 1 mV/s. The electrochemical tests were performed at 37°C.

3. Results and Discussion

Raman scattering spectroscopy evaluated the chemical structure of the DLC films. Two broad bands compose the spectra for visible light, one centered in ~1330 cm^{-1} (D band) and other in ~1530 cm^{-1} (G band) [25]. The D and G band positions were determined by subtracting a linear background and fitting a Gaussian function to the peak of the Raman spectrum (Figure 1). Table 1 summarizes the main parameters obtained through the spectra. The bond stretching of all pairs of sp^2 atoms in both rings and chains causes the G band [26, 27]. The breathing modes of sp^2 atoms in rings caused the D band and appears only in the presence of defects [26, 27]. The TiO_2-DLC films presented a shift in D and G band positions towards higher wavenumbers. The full width at half maximum (FWHM) of G band measures structural disorder and arises from bond length distortions [27]. The presence of TiO_2 nanoparticles in DLC films results in the increase of the intensity ratio of D and G area (A_D/A_G) and a shift of D and

Table 1: Gaussian fitting results of Raman spectra from DLC and TiO_2-DLC films.

TiO_2 concentration (g/L)	D band position (cm^{-1})	G band position (cm^{-1})	FWHM (D)	FWHM (G)	A_D/A_G	$FWHM_D/FWHM_G$
0.0	1330.1	1531.1	296.7	154.2	0.51	1.92
0.1	1354.4	1552.3	298.4	144.9	0.81	2.06
0.5	1334.4	1531.4	333.0	162.2	0.67	2.05

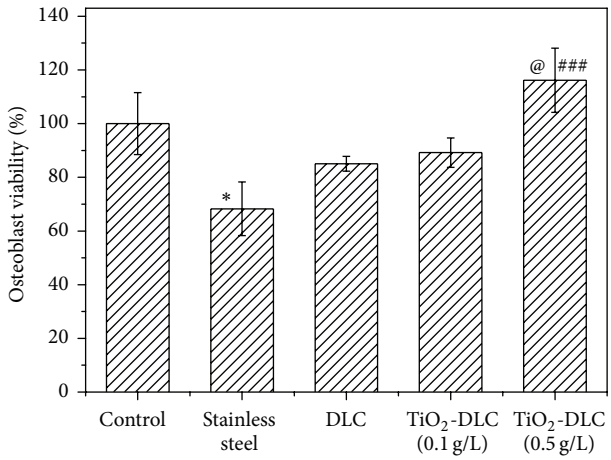

Figure 2: Osteoblast viability assessed by MTT assay in cells cultured for 24 h on stainless steel, DLC, and TiO_2-DLC surfaces. The percentage was calculated by normalization of optical density to the control (osteoblast cells). Results are shown as average ± standard error for $n = 5$ (one-way ANOVA and Tukey's multiple comparisons test). Control: osteoblasts plated on plastic surfaces. $^{*}P < 0.05$: the interaction is considered significant compared to control (osteoblast cells); $^{\#\#\#}P < 0.001$: the interaction is considered extremely significant compared to stainless steel (noncoated substrate); $^{@}P < 0.05$: the interaction is considered significant compared to DLC (coating without any nanoparticle).

G bands towards higher wave numbers. These characteristics imply the increase of the graphite-like bonds in DLC matrix [26–28].

In this study, mouse osteoblastic cells were the cell culture system. Calvaria cells have a high proliferation capacity, being able to expand *in vitro*, which is appropriate to study interactions with biomaterials [29].

The MTT assay is a quantitative method for evaluating a cell response to external factors. It measures the reduction of a tetrazolium component (MTT) into an insoluble formazan product by NAD(P)H-dependent oxidoreductase enzymes, largely in the cytosolic compartment of the cell, specifically in mitochondrial compartment. The mitochondrial enzyme succinate-dehydrogenase within viable cells is able to cleave the tetrazolium salt into a blue product (formazan). The color produced is directly proportional to the number of viable cells [30].

Figure 2 shows the mitochondrial activity for all the studied samples. Stainless steel shows a significant difference when compared to control (osteoblast cells). The decrease number of viable cells on stainless steel characterizes cell death. There was no significant difference among DLC, TiO_2-DLC (0.1 g/L), and the control. An increased concentration of TiO_2 nanoparticles (0.5 g/L) in DLC films raised the mitochondrial activity on these samples, which are obviously nontoxic. TiO_2-DLC (0.5 g/L) is significantly different ($P < 0.05$) compared to DLC and extremely significant ($P < 0.001$) when compared to stainless steel.

DAPI (blue) labeled the cell nuclei during 24 h (Figure 3). All the TiO_2-DLC samples had a high cell attachment. The DAPI test showed a strong compatibility of the TiO_2-DLC films. Figure 4 shows the counted osteoblast cells adhered on the samples. The number of cells on stainless steel is considered different from DLC films ($P < 0.05$) and very different from TiO_2-DLC films ($P < 0.01$). There was an increase in cells according to the increased concentration of TiO_2 in DLC films. TiO_2-DLC films are considered different from DLC films ($P < 0.05$).

The study of bone metabolism and biomaterial/cell, which is essential for bone tissue engineering, generally uses osteoblasts [29]. However, not only cell adhesiveness and toxicity have to be investigated to design biomaterials. The existence of interface phenomena can affect the initial proliferation and cell recruitment at the biomaterial surface [31]. The hydrophilicity tries to obtain correlation between cell response and the biomaterial surface [29].

Table 2 shows the contact angles of the samples formed with distilled water and diiodomethane. As the concentration of TiO_2 nanoparticles in DLC films increased, the water contact angle decreased from 82 to ~53°, and in the case of diiodomethane, the contact angle had a slight increase. Usually, a hydrophobic surface has a contact angle higher than 70°, while a hydrophilic surface has a contact angle lower than 70° [32]. These results indicate that TiO_2-DLC is hydrophilic. This characteristic may be derivate from the amorphous TiO_2 surfaces [33].

Table 2 also lists the surface energy components according to the Owens method [22]. Dispersive ($\gamma_d = 36.1$ mN/m) and polar ($\gamma_p = 3.6$ mN/m) components gave the total surface energy (γ) of 40.0 mN/m for the as-deposited DLC. The interfacial free energy settles the wetting and so the wall shear stress when the liquid touches the surface [22]. As the concentration of TiO_2 in DLC increased, the total surface energy had a slight increase. The increasing in the polar component (a quantitative indicator of hydrophilicity) increases the total surface energy of TiO_2-DLC. Oxide particles cause a higher polar component on TiO_2-DLC surface [34]. The polar component attracts the electric dipole of water, which minimizes the interfacial energy and the water contact angle [34]. The water contact angle decreased as the

Table 2: Contact angle and surface energy components of DLC and TiO_2-DLC films. Each mean value corresponds to the average value on five different areas.

Concentration of TiO_2 nanoparticles (g/L)	Contact angle, θ (°)		Surface energy components (mN/m)			Work of adhesion (mJ/m^2)
	Water	Diiodomethane	Dispersive	Polar	Total	
0.0	82.0 ± 4.7	38.5 ± 1.0	36.1 ± 1.5	3.6 ± 1.9	40.0 ± 3.3	−6.6
0.1	72.1 ± 4.7	42.7 ± 1.5	31.1 ± 1.4	9.5 ± 2.8	40.6 ± 4.2	−8.5
0.5	53.3 ± 1.5	44.1 ± 5.4	27.4 ± 0.9	22.5 ± 4.1	49.9 ± 5.0	−14.4

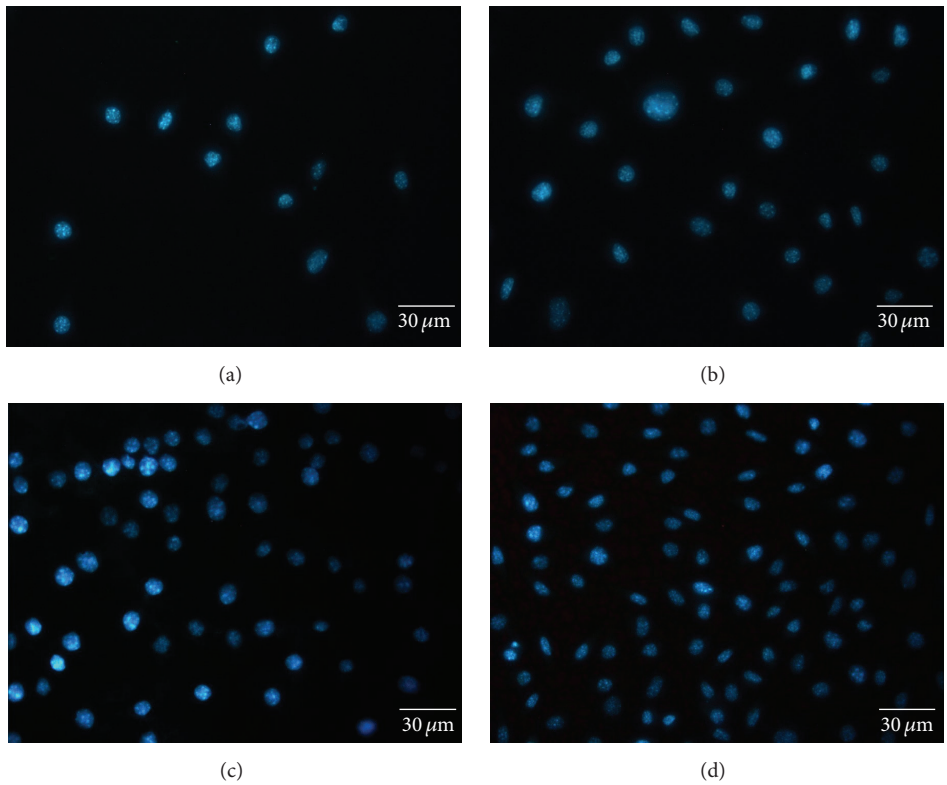

Figure 3: Fluorescence images from osteoblast cell nuclei on (a) stainless steel, (b) DLC, (c) TiO_2-DLC (0.1 g/L), and (d) TiO_2-DLC (0.5 g/L) films labeled with DAPI (blue) at 24 h.

polar component in the surface energy increased. The polar component attracts electric dipole of water molecule, which reduces the interfacial energy between the surface and the water and, thus, the wetting angle of water [35].

A thermodynamic approach offers a powerful tool to predict cell spreading to solids [36, 37]. For this, the surface free energy values of the cells (γ_C) calculated by Schakenraad et al. [23] were used. Table 2 lists the average values of work of adhesion (W_{Ad}) for the studied samples. All the calculated values for W_{Ad} for cell adhesion on DLC and TiO_2-DLC films are negative. W_{Ad} point out favorable conditions for cell adhesion, as provided by Schakenraad et al. [23]. In addition, as the TiO_2 concentration increases, W_{Ad} values became more negative. This result suggests that as the TiO_2 content in DLC films increased, DLC films became more thermodynamically favorable to cell spreading.

Figure 5 shows the correlation between the number of cells on the samples (Figure 4) and the calculated work of adhesion (Table 2). Besides the fact that there are two independent results, this comparison corroborates that TiO_2 content increased the cell adhesion on DLC films.

However, one of the physical characteristics that settle the implant corrosion is the thermodynamic force [38, 39]. It causes corrosion by either oxidation or reduction reaction [38, 39]. Oral liquids, like saliva, attacks the metallic implants causing the dissolution of them [38]. Therefore, the release of metallic ions caused by corrosion also affects the biocompatibility of the implant. The potentiodynamic polarization test assessed the corrosion susceptibility of the metallic implant in artificial saliva. Figure 6 shows the potentiodynamic curves for stainless steel, DLC, and TiO_2-DLC films. Table 3 summarizes the electrochemical parameters obtained from the potentiodynamic polarization curves (Figure 6).

The penetration of the test solution causes the negative open circuit potential values [40]. TiO_2-DLC (0.1 g/L) films presented the greatest E_{corr} value (−0.146 mV) in potentiodynamic polarization test. The corrosion current density (i_{corr}) reduced from 1.72 to 0.054 nA/cm^2 and the protection

Table 3: Electrochemical parameters obtained from potentiodynamic polarization curves.

Samples	E_{corr} (mV)	i_{corr} (nA/cm^2)	Protective efficiency (%)
Stainless steel	−0.495	117	—
DLC	−0.419	1.72	98.5
TiO_2-DLC (0.1 g/L)	−0.146	0.151	99.9
TiO_2-DLC (0.5 g/L)	−0.220	0.054	100.0

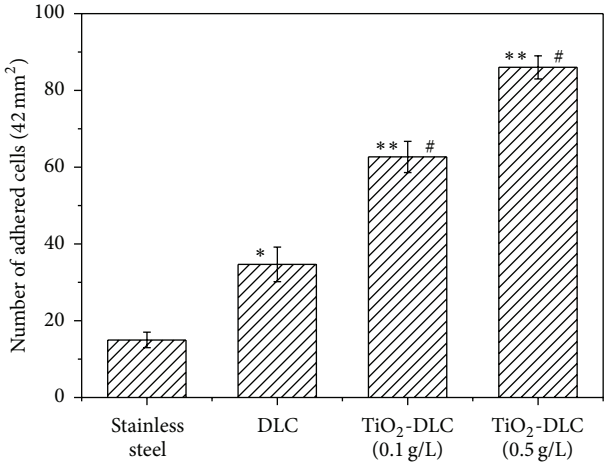

Figure 4: Number of adhered cells labeled with DAPI (blue) at 24 h. Results are shown as average ± standard error for $n = 3$ (one-way ANOVA and Tukey's multiple comparisons test). $^*P < 0.05$: the interaction is considered significant compared to stainless steel (substrate without coating); $^{**}P < 0.01$: the interaction is considered very significant compared to stainless steel; $^{\#}P < 0.05$: the interaction is considered significant compared to DLC (coating without any nanoparticle).

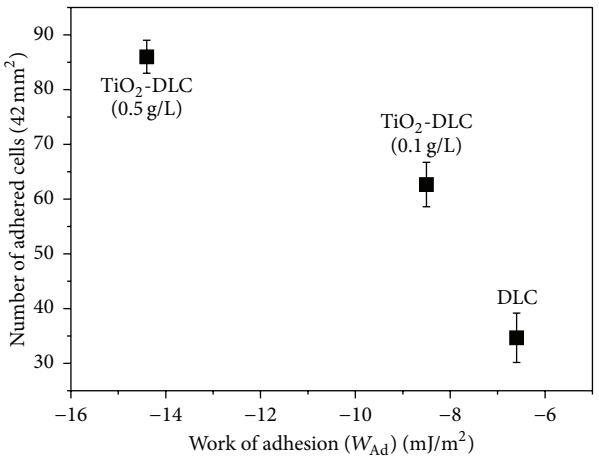

Figure 5: Number of osteoblast cells on the samples versus the interfacial free energy of adhesion of DLC and TiO_2-DLC films.

efficiency [41] increased from 98.5 to 100.0% with the increase of TiO_2 content. Lower current density and higher potential generally points out better corrosion resistance. The shift in the polarization curve towards the region of lower current

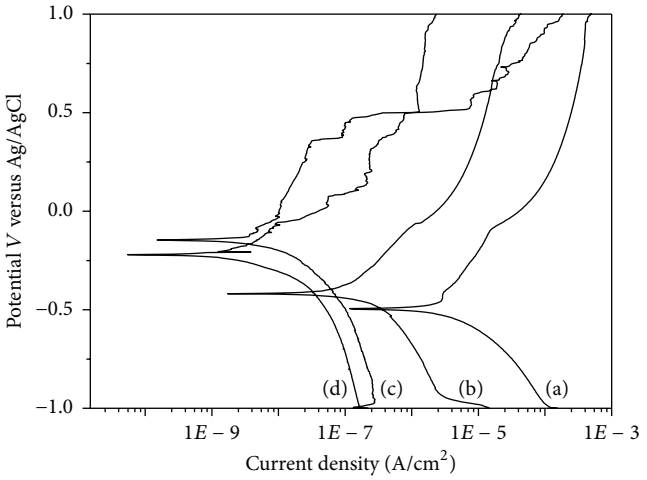

Figure 6: Potentiodynamic polarization curves from (a) stainless steel uncoated and coated with (b) DLC, (c) TiO_2-DLC (0.1 g/L), and (d) TiO_2-DLC (0.5 g/L) films.

density and higher potential is an indicative of the increased corrosion protection with the increased TiO_2 concentration.

The difference in the film microstructure assigns different corrosion behaviors [42]. The comparison between electrochemical parameters (Table 3) and chemical structure (Table 1) shows a tendency to reduce the corrosion current density of the samples as the film disorder increase. Robertson [43] states sp^3 bonding of DLC confers on it many of the valuable properties of diamond itself, such as its chemical and electrochemical inertness. Generally, the higher the sp^3/sp^2 ratio, the higher the electrochemical corrosion resistance [44].

4. Conclusion

In this paper, the osteoblast attachment and spreading on DLC coatings was studied when TiO_2 nanoparticles are incorporated. The presence of TiO_2 nanoparticles increases the graphite-like bonds and decreases the DLC disorder. As TiO_2 increased, the films increased the osteoblast viability (MTT assay), becoming more thermodynamically favorable to cell spreading (W_{Ad} values became more negative). This was evidenced through the increasing number of osteoblast nuclei suggesting a higher adhesion between the cells and the films. The potentiodynamic polarization test in artificial saliva shows an increase in corrosion protection with the increased TiO_2. These results show the potential use of TiO_2-DLC films in implantable surfaces for dental applications.

Competing Interests

The authors declare that they have no competing interests.

Acknowledgments

The authors thank Professor Dr. Rosilene Fernandes da Rocha and Dr. Isabel Chaves Silva Carvalho from School of Dentistry, Paulista State University, São José dos Campos, Brazil, for kindly providing the cells from newborn Wistar rat calvaria and Sao Paulo Research Foundation, FAPESP (2011/17877-7), (2011/20345-7), (2012/15857-1), and (2013/20054-8) for the financial support.

References

[1] M. Zafar, S. Najeeb, Z. Khurshid et al., "Potential of electrospun nanofibers for biomedical and dental applications," *Materials*, vol. 9, no. 2, article 73, 2016.

[2] E. Salgueiredo, M. Vila, M. A. Silva et al., "Biocompatibility evaluation of DLC-coated Si3N4 substrates for biomedical applications," *Diamond and Related Materials*, vol. 17, no. 4-5, pp. 878–881, 2008.

[3] J. Robertson, "Diamond-like amorphous carbon," *Materials Science and Engineering: R: Reports*, vol. 37, no. 4–6, pp. 129–282, 2002.

[4] C. Donnet, J. Fontaine, T. Le Mogne et al., "Diamond-like carbon-based functionally gradient coatings for space tribology," *Surface & Coatings Technology*, vol. 120-121, pp. 548–554, 1999.

[5] D. Y. Yun, W. S. Choi, Y. S. Park, and B. Hong, "Effect of H_2 and O_2 plasma etching treatment on the surface of diamond-like carbon thin film," *Applied Surface Science*, vol. 254, no. 23, pp. 7925–7928, 2008.

[6] A. Shirakura, M. Nakaya, Y. Koga, H. Kodama, T. Hasebe, and T. Suzuki, "Diamond-like carbon films for PET bottles and medical applications," *Thin Solid Films*, vol. 494, no. 1-2, pp. 84–91, 2006.

[7] R. Hauert, "A review of modified DLC coatings for biological applications," *Diamond and Related Materials*, vol. 12, no. 3–7, pp. 583–589, 2003.

[8] M. Ban and N. Hasegawa, "Deposition of diamond-like carbon thin films containing photocatalytic titanium dioxide nanoparticles," *Diamond and Related Materials*, vol. 25, pp. 92–97, 2012.

[9] Q. Zhao, Y. Liu, C. Wang, and S. Wang, "Bacterial adhesion on silicon-doped diamond-like carbon films," *Diamond and Related Materials*, vol. 16, no. 8, pp. 1682–1687, 2007.

[10] W. J. Ma, A. J. Ruys, R. S. Mason et al., "DLC coatings: effects of physical and chemical properties on biological response," *Biomaterials*, vol. 28, no. 9, pp. 1620–1628, 2007.

[11] T. Yokota, T. Terai, T. Kobayashi, T. Meguro, and M. Iwaki, "Cell adhesion to nitrogen-doped DLCs fabricated by plasma-based ion implantation and deposition method using toluene gas," *Surface & Coatings Technology*, vol. 201, no. 19-20, pp. 8048–8051, 2007.

[12] E. Eisenbarth, D. Velten, K. Schenk-Meuser et al., "Interactions between cells and titanium surfaces," *Biomolecular Engineering*, vol. 19, no. 2–6, pp. 243–249, 2002.

[13] H. Nakano, N. Hasuike, K. Kisoda, K. Nishio, T. Isshiki, and H. Harima, "Synthesis of TiO_2 nanocrystals controlled by means of the size of magnetic elements and the level of doping with them," *Journal of Physics Condensed Matter*, vol. 21, no. 6, Article ID 064214, 2009.

[14] P. C. Maness, S. Smolinski, D. M. Blake, Z. Huang, E. J. Wolfrum, and W. A. Jacoby, "Bactericidal activity of photocatalytic TiO_2 reaction: toward an understanding of its killing mechanism," *Applied and Environmental Microbiology*, vol. 65, no. 9, pp. 4094–4098, 1999.

[15] F. R. Marciano, D. A. Lima-Oliveira, N. S. Da-Silva, A. V. Diniz, E. J. Corat, and V. J. Trava-Airoldi, "Antibacterial activity of DLC films containing TiO_2 nanoparticles," *Journal of Colloid and Interface Science*, vol. 340, no. 1, pp. 87–92, 2009.

[16] F. R. Marciano, C. C. Wachesk, A. O. Lobo, V. J. Trava-Airoldi, C. Pacheco-Soares, and N. S. Da-Silva, "Thermodynamic aspects of fibroblastic spreading on diamond-like carbon films containing titanium dioxide nanoparticles," *Theoretical Chemistry Accounts*, vol. 130, no. 4, pp. 1085–1093, 2011.

[17] C. C. Wachesk, C. A. F. Pires, B. C. Ramos et al., "Cell viability and adhesion on diamond-like carbon films containing titanium dioxide nanoparticles," *Applied Surface Science*, vol. 266, pp. 176–181, 2013.

[18] M. Saini, Y. Singh, P. Arora, V. Arora, and K. Jain, "Implant biomaterials: a comprehensive review," *World Journal of Clinical Cases*, vol. 3, no. 1, pp. 52–57, 2015.

[19] Z. Khurshid, M. Zafar, S. Qasim, S. Shahab, M. Naseem, and A. AbuReqaiba, "Advances in nanotechnology for restorative dentistry," *Materials*, vol. 8, no. 2, pp. 717–731, 2015.

[20] A. S. Litsky, "Clinical reviews: bioabsorbable implants for orthopaedic fracture fixation," *Journal of Applied Biomaterials*, vol. 4, no. 1, pp. 109–111, 1993.

[21] P. T. de Oliveira and A. Nanci, "Nanotexturing of titanium-based surfaces upregulates expression of bone sialoprotein and osteopontin by cultured osteogenic cells," *Biomaterials*, vol. 25, no. 3, pp. 403–413, 2004.

[22] D. K. Owens and R. C. Wendt, "Estimation of the surface free energy of polymers," *Journal of Applied Polymer Science*, vol. 13, no. 8, pp. 1741–1747, 1969.

[23] J. M. Schakenraad, H. J. Busscher, C. R. H. Wildevuur, and J. Arends, "Thermodynamic aspects of cell spreading on solid substrata," *Cell Biophysics*, vol. 13, no. 1, pp. 75–91, 1988.

[24] J. Geis-Gerstorfer and H. Weber, "Effect of potassium thiocyanate on corrosion behavior of non-precious metal dental alloys," *Deutsche zahnarztliche Zeitschrift*, vol. 40, no. 2, pp. 87–91, 1985.

[25] F. Tuinstra and J. L. Koenig, "Raman spectrum of graphite," *Journal of Chemical Physics*, vol. 53, no. 3, pp. 1126–1130, 1970.

[26] C. Casiraghi, F. Piazza, A. C. Ferrari, D. Grambole, and J. Robertson, "Bonding in hydrogenated diamond-like carbon by Raman spectroscopy," *Diamond and Related Materials*, vol. 14, no. 3–7, pp. 1098–1102, 2005.

[27] L. Ji, H. X. Li, F. Zhao, J. M. Chen, and H. D. Zhou, "Microstructure and mechanical properties of Mo/DLC nanocomposite films," *Diamond and Related Materials*, vol. 17, no. 11, pp. 1949–1954, 2008.

[28] A. Madhan Kumar and N. Rajendran, "Electrochemical aspects and in vitro biocompatibility of polypyrrole/TiO_2 ceramic nanocomposite coatings on 316L SS for orthopedic implants," *Ceramics International*, vol. 39, no. 5, pp. 5639–5650, 2013.

[29] C. Wirth, B. Grosgogeat, C. Lagneau, N. Jaffrezic-Renault, and L. Ponsonnet, "Biomaterial surface properties modulate *in vitro* rat calvaria osteoblasts response: roughness and or chemistry?" *Materials Science & Engineering C—Biomimetic and Supramolecular Systems*, vol. 28, no. 5-6, pp. 990–1001, 2008.

[30] H. Wan, R. Williams, P. Doherty, and D. F. Williams, "A study of the reproducibility of the MTT test," *Journal of Materials Science: Materials in Medicine*, vol. 5, no. 3, pp. 154–159, 1994.

[31] J. Pino-Mínguez, A. Jorge-Mora, R. Couceiro-Otero, and C. García-Santiago, "Study of the viability and adhesion of osteoblast cells to bone cements mixed with hydroxyapatite at different concentrations to use in vertebral augmentation techniques," *Revista Española de Cirugía Ortopédica y Traumatología (English Edition)*, vol. 59, no. 2, pp. 122–128, 2015.

[32] H. W. Choi, R. H. Dauskardt, S.-C. Lee, K.-R. Lee, and K. H. Oh, "Characteristic of silver doped DLC films on surface properties and protein adsorption," *Diamond and Related Materials*, vol. 17, no. 3, pp. 252–257, 2008.

[33] A. Sobczyk-Guzenda, M. Gazicki-Lipman, H. Szymanowski et al., "Characterization of thin TiO_2 films prepared by plasma enhanced chemical vapour deposition for optical and photocatalytic applications," *Thin Solid Films*, vol. 517, no. 18, pp. 5409–5414, 2009.

[34] R. K. Roy, H. W. Choi, J. W. Yi et al., "Hemocompatibility of surface-modified, silicon-incorporated, diamond-like carbon films," *Acta Biomaterialia*, vol. 5, no. 1, pp. 249–256, 2009.

[35] R. K. Roy, H.-W. Choi, S.-J. Park, and K.-R. Lee, "Surface energy of the plasma treated Si incorporated diamond-like carbon films," *Diamond and Related Materials*, vol. 16, no. 9, pp. 1732–1738, 2007.

[36] E. Flahaut, M. C. Durrieu, M. Remy-Zolghadri, R. Bareille, and C. Baquey, "Investigation of the cytotoxicity of CCVD carbon nanotubes towards human umbilical vein endothelial cells," *Carbon*, vol. 44, no. 6, pp. 1093–1099, 2006.

[37] S. M. Hussain, K. L. Hess, J. M. Gearhart, K. T. Geiss, and J. J. Schlager, "In vitro toxicity of nanoparticles in BRL 3A rat liver cells," *Toxicology in Vitro*, vol. 19, no. 7, pp. 975–983, 2005.

[38] J. J. Jacobs, J. L. Gilbert, and R. M. Urban, "Corrosion of metal orthopaedic implants," *The Journal of Bone & Joint Surgery—American Volume*, vol. 80, no. 2, pp. 268–282, 1998.

[39] J. J. Jacobs, R. M. Latanision, R. M. Rose, and S. J. Veeck, "The effect of porous coating processing on the corrosion behavior of cast Co-Cr-Mo surgical implant alloys," *Journal of Orthopaedic Research*, vol. 8, no. 6, pp. 874–882, 1990.

[40] C. L. Liu, M. Xu, W. Zhang, S. H. Pu, and P. K. Chu, "Effects of tungsten pre-implanted layer on corrosion and electrochemical characteristics of amorphous carbon films on stainless steel," *Diamond and Related Materials*, vol. 17, no. 7–10, pp. 1738–1742, 2008.

[41] H.-G. Kim, S.-H. Ahn, J.-G. Kim, S. J. Park, and K.-R. Lee, "Electrochemical behavior of diamond-like carbon films for biomedical applications," *Thin Solid Films*, vol. 475, no. 1-2, pp. 291–297, 2005.

[42] Z. Wang, C. Wang, Q. Wang, and J. Zhang, "Electrochemical corrosion behaviors of a-C:H and a-C:N_X:H films," *Applied Surface Science*, vol. 254, no. 10, pp. 3021–3025, 2008.

[43] J. Robertson, "Diamond-like amorphous carbon," *Materials Science and Engineering: R: Reports*, vol. 37, no. 4–6, pp. 129–281, 2002.

[44] A. Dorner-Reisel, C. Schürer, G. Irmer, and E. Müller, "Electrochemical corrosion behaviour of uncoated and DLC coated medical grade Co28Cr6Mo," *Surface and Coatings Technology*, vol. 177-178, pp. 830–837, 2004.